




Article

Assessing the Effects of Irrigation Water Salinity on Two Ornamental Crops by Remote Spectral Imaging

Xinyang Yu ^{1,2}, Younggu Her ^{1,*} , Anjin Chang ³, Jung-Hun Song ¹ , E. Vanessa Campoverde ⁴ and Bruce Schaffer ⁵ 

¹ Tropical Research and Education Center, Department of Agricultural and Biological Engineering, Institute of Food and Agricultural Sciences, University of Florida, Homestead, FL 33031, USA; x.yu@ufl.edu or yuxinyang19860915@163.com (X.Y.); junghunsong@ufl.edu (J.-H.S.)

² Department of Land Resource and Information Technology, College of Resources and Environment, Shandong Agricultural University, Tai'an City 271001, China

³ School of Engineering and Computing Science, Texas A&M University-Corpus Christi, Corpus Christi, TX 78412, USA; Anjin.Chang@tamucc.edu

⁴ UF/IFAS Extension Miami-Dade County, Institute of Food and Agricultural Sciences, University of Florida, Homestead, FL 33030, USA; evcampoverde@ufl.edu

⁵ Tropical Research and Education Center, Department of Horticultural Sciences, Institute of Food and Agricultural Sciences, University of Florida, Homestead, FL 33031, USA; bas56@ufl.edu

* Correspondence: yher@ufl.edu; Tel.: +1-786-217-9288



Citation: Yu, X.; Her, Y.; Chang, A.; Song, J.-H.; Campoverde, E.V.; Schaffer, B. Assessing the Effects of Irrigation Water Salinity on Two Ornamental Crops by Remote Spectral Imaging. *Agronomy* **2021**, *11*, 375. <https://doi.org/10.3390/agronomy11020375>

Academic Editor: Jesus Ochoa and María José Gómez-Bellot

Received: 29 January 2021
Accepted: 15 February 2021
Published: 20 February 2021

Publisher's Note: MDPI stays neutral with regard to jurisdictional claims in published maps and institutional affiliations.



Copyright: © 2021 by the authors. Licensee MDPI, Basel, Switzerland. This article is an open access article distributed under the terms and conditions of the Creative Commons Attribution (CC BY) license (<https://creativecommons.org/licenses/by/4.0/>).

Abstract: Salinity is one of the most common and critical environmental factors that limit plant growth and reduce crop yield. The aquifers, the primary sources of irrigation water, of south Florida are shallow and highly permeable, which makes agriculture vulnerable to projected sea level rise and saltwater intrusion. This study evaluated the growth responses of two ornamental nursery crops to the different salinity levels of irrigation water to help develop saltwater intrusion mitigation plans for the improved sustainability of the horticultural industry in south Florida. Two nursery crops, *Hibiscus rosa-sinensis* and *Mandevilla splendens*, were treated with irrigation water that had seven different salinity levels from 0.5 (control) to 10.0 dS/m in the experiment. Crop height was measured weekly, and growth was monitored daily using the normalized difference vegetation index (NDVI) values derived from multispectral images collected using affordable sensors. The results show that the growth of *H. rosa-sinensis* and *M. splendens* was significantly inhibited when the salinity concentrations of irrigation water increased to 7.0 and 4.0 dS/m, for each crop, respectively. No significant differences were found between the NDVI values and plant growth variables of both *H. rosa-sinensis* and *M. splendens* treated with the different irrigation water salinity levels less than 2.0 dS/m. This study identified the salinity levels that could reduce the growth of the two nursery crops and demonstrated that the current level of irrigation water salinity (0.5 dS/m) would not have significant adverse effects on the growth of these crops in south Florida.

Keywords: salinity; irrigation; ornamental crop; remotely sensed images; south Florida; saltwater intrusion

1. Introduction

South Florida's subtropical marine climate is conducive to growing a wide variety of subtropical and tropical ornamental crops year-round. Miami-Dade County ranks as the number one ornamental crop production area in Florida, with 76% of the total amount of ornamental crops produced commercially in the U.S. [1]. However, these favorable environmental conditions are also ideal for a high constant groundwater extraction that poses a challenge of saltwater intrusion into freshwater wells. In addition, reclaimed water from wastewater treatment facilities has become the source of landscape irrigation in Florida and California [2,3]. Therefore, irrigation water quality is an important aspect of horticultural production in more than 1300 nurseries in south Florida [4].

The aquifer systems in Florida have been experiencing saltwater intrusion caused by sea level rise, leading to the contamination of wells for agricultural and domestic water supplies and changes in water management practices in south Florida [5–7]. The aquifers are shallow and highly permeable, making agriculture in south Florida very vulnerable to sea level rise and saltwater intrusion. In Miami-Dade County, 1640.5 million liters (c.f., 92.6 million liters from surface water sources) of freshwater are withdrawn from the aquifers each day, and irrigation water is taken from groundwater sources at a rate of 226.8 million liters (c.f., 24.9 million gallons from surface water sources) per day [8].

Salinity has a critical negative impact on crop growth and yield. The high salinity levels of irrigation water can cause plant stress; the level of salt stress depends on the crop species, the frequency and length of exposure, and the salinity level. Best management practices (BMPs) for ornamental crop production in south Florida involve the utilization of good quality water and mitigation of environmental factors that can decrease the growth and quality of crops, especially during hurricanes and tropical storms that are common in south Florida. Studies have shown that large storm events could bring the storm surge along the low-lying open coastal areas such as south Florida's shorelines and result in seawater intruding onto the inland ground surface [9,10]. The intruded saltwater could infiltrate into the porous soil layers and then further percolate into the freshwater aquifer. During Hurricane Maria in 2017, many plant nurseries were concerned about saltwater intrusion in surface and subsurface water bodies and potential salt stress to their crops, particularly because there is little information on plant responses to salinity levels in irrigation water used for ornamental crop production. Evaluating the effects of salinity levels in irrigation water on the growth and production of nursery crops in south Florida would provide valuable information for irrigation management in the face of changing salinity levels in south Florida's water supply.

Remote sensing data and techniques have been widely used to monitor the changes in the physical and physiological traits and characteristics of crops over time [11–13]. Remote sensing technologies are also getting more affordable and feasible, with various sensors that can provide finer spatiotemporal resolutions and broader spectral coverage of images for crop monitoring [14–16]. Studies have found that the visible spectrum of remotely sensed images could be closely associated with above-ground biomass [17,18], and visible-near infrared spectroscopy can be used to identify physiological changes in plants induced by water, nutrient stresses, and field management [19–21]. For improved accuracy of monitoring crop vigor represented by canopy greenness [22,23] and above-ground biomass [24,25], studies have employed remote sensors that have fine spatial and spectral resolutions [26,27]. However, crop growth monitoring has been conducted on a monthly, seasonally, and even yearly basis. The opportunity to collect remotely sensed data from a space- or airborne platform is limited for crop monitoring. Plot-scale remote sensing techniques, including tower-mounted or unmanned aircraft systems (UASs), have been widely adopted to remotely collect data about crop growth and provide the data at fine temporal and spatial resolutions [28–32].

Hibiscus rosa-sinensis and *Mandevilla splendens* are economically important nursery crops widely planted in south Florida. *H. rosa-sinensis* is a tropical hibiscus species in the *Hibisceae* tribe of the *Malvaceae* family (Figure 1b,c). It is a bushy, evergreen shrub or small tree with glossy leaves and brilliant red five-petaled flowers. *M. splendens* is a flowering vine plant in the dogbane family, *Apocynaceae* (Figure 1c). It has wide green glossy leaves of elliptical or rectangular shape growing to 20 cm long. These two tropical plants are known not to tolerate temperatures below 10 °C (50 °F) [33,34].

The objectives of this study were to assess the impacts of irrigation salinity on two economically critical ornamental crops commonly produced in south Florida, *H. rosa-sinensis* and *M. splendens*, and to identify the level of salinity that can significantly reduce their vigor and growth. To accomplish the objectives, we monitored how the crop growth reacts to the different salinity concentrations of irrigation water using remotely sensed images and crop growth variables such as biomass, crop height, and width.

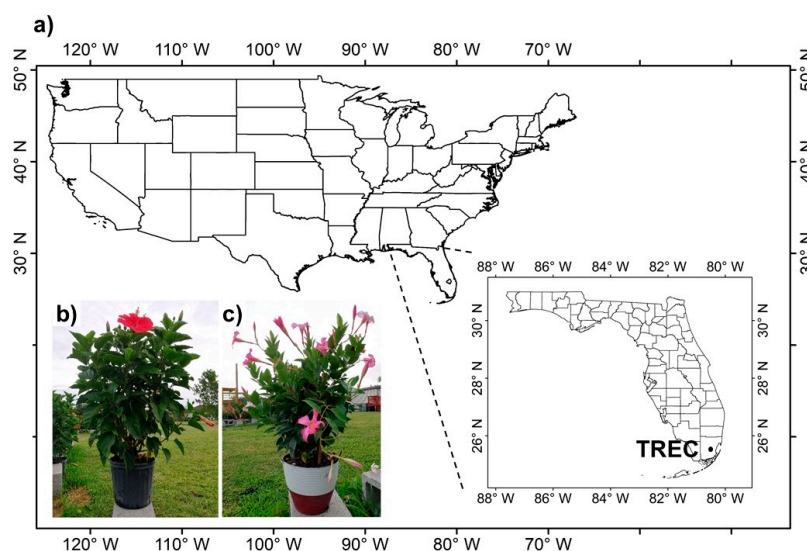


Figure 1. Location of the experiment site and crops investigated in this study. (a) The location of the Tropical Research and Education Center (TREC), University of Florida, Homestead, Florida; (b) *H. rosa-sinensis*; (c) *M. splendens*.

2. Materials and Methods

2.1. Experimental Setup

This study was conducted at the UF/IFAS Tropical Research and Education Center (TREC; latitude: 25°30'24" N, longitude: 80°29'58" W) in Homestead, FL (Figure 1a). During the experiments, weather data (air temperature, relative humidity, precipitation, and wind speed) were collected automatically by the Florida Automatic Weather Network (FAWN) station located at TREC (<https://fawn.ifas.ufl.edu/station.php?id=440> (accessed on 9 December 2019)). The *H. rosa-sinensis* and *M. splendens* plants investigated in this study were provided by a local nursery, Costa Farms® (<http://www.costafarms.com/> (accessed on 15 December 2020)). The potting medium was the standard mix that the nursery used (Atlas Peat & Soil, Inc., Boynton Beach, FL 33472, USA).

H. rosa-sinensis and *M. splendens* were each treated with seven different levels of irrigation water salinity, including 0.5 (control, which is the current level generally found in south Florida's irrigation water), 1.0 (denoted as T1), 1.5 (T2), 2.0 (T3), 4.0 (T4), 7.0 (T5), and 10.0 dS/m (T6). The treatments were grouped into two experiments; the first experiment was conducted with the salinity levels of 1.0, 1.5, and 2.0 dS/m that are less than 200% of the control. In the second experiment, the salinity levels were increased to 4.0, 7.0, and 10.0 dS/m based on the results of the first experiment. Each experiment was arranged in a completely randomized design with four single-plant replicates per treatment for each species.

Irrigation and management practices, including water application timing and rates, during the experiment were the same as those used by local nurseries, so that results can be directly applicable to the local nursery industry. For example, 1.89 L of water were applied to *H. rosa-sinensis* twice a day at 8 a.m. and 5 p.m. (or a total of 3.96 L of water were applied to *H. rosa-sinensis* a day). In the case of *M. splendens*, 0.95 L of water were applied every two days (at 5 p.m.). The sizes (volumes) of pots used to grow *H. rosa-sinensis* and *M. splendens* were 8.0 L and 3.6 L, respectively. The fertilizers, 18-6-8 (N-P-K, granular, slow release, Nutricote® Controlled Release Fertilizer, Chisso-Asahi Fertilier Co., LTD: 7-12 Kouraku 1-chome, Bunkyo-ku, Japan) and 24-8-16 (N-P-K, granular, fast release, Miracle-Gro® Water Soluble All Purpose Plant Food, the Scotts company: 14111 Scottslawn Road, Marysville, OH 43041, USA), were applied to *H. rosa-sinensis* (15 g per pot) and *M. splendens* (10 g per pot) every week.

The salinity levels of irrigation water were determined based on those of groundwater (or the source of irrigation water in south Florida) reported in the literature and a prelimi-

nary salinity analysis of local irrigation water [35,36]. For instance, a USGS groundwater salinity monitoring station close to the study area (Station ID: 254335080170501) showed that the salinity of groundwater could increase up to 9.12 dS/m depending on the depths (from the ground surface to 30 m) and seasons [37]. Ten bottles (100 mL) of water were collected at the outlets of sprinklers located in a local nursery farm (Costa Farms in Homestead, FL, USA), and a lab test showed that the irrigation water had a salinity level of 0.50 dS/m on average with a standard deviation of 0.03 dS/m.

Irrigation water used in the experiments was pumped out of a groundwater well located next to the study site at TREC, and the salinity level of the well water was 0.55 dS/m. The pumped water was then stored in four 20-gallon applicator sump tanks constructed from medium-density polyethylene with ultraviolet inhibitors in each experiment. The different salinity levels were obtained by adding sodium chloride (NaCl, CAS No.: 7647-14-5, Minimum Assay of 99.0%) to irrigation water stored in the sump tanks. The salinity concentrations were measured using a salinity meter (edge[®] Multiparameter EC/TDS/Salinity Meter, H12030-01, HANNA Instruments: 270 George Washington Hwy., Smithfield, RI 02917, USA) calibrated with the conductivity standards of 700 $\mu\text{S}/\text{cm}$ and 2000 $\mu\text{Mho}/\text{cm}$ (ID No. 97J-00D-K1, SF1318B and SF1319B).

2.2. Plant Growth Variables Monitoring

Each crop's height and width were measured once every week to monitor their growth rates. At the end of the experiment, all the plants were harvested, and the leaves and stems were separated from the roots. The separated plant tissues were dried for 24 h to constant weights, and the above-ground biomass was measured. Two statistics were employed to measure the growth rates: the relative and intrinsic growth rates. The relative growth rate (RGR) was calculated as described by Hilbert et al. [38] and Radford [39]:

$$RGR = \frac{\ln H_2 - \ln H_1}{t_2 - t_1}, \quad (1)$$

where H_i is the height of crops in the i th week, and t_i represents the i th week. The crop height measurements were fitted to the standard form (i.e., sigmoidal curve) of logistic growth curves to calculate the intrinsic growth rates [40–44]:

$$H_t = \frac{K}{1 + \left(\frac{K-H_0}{H_0}\right)e^{-rt}}, \quad (2)$$

where H_0 is the crop size (height) at the beginning of the growth curve, K is the final crop height in a particular environment, and r is the intrinsic growth rate (IGR) of the crop that would occur if there were no restrictions imposed on crop growth. The nonlinear least-squares Levenberg–Marquardt algorithm was used to identify the intrinsic growth rate value that makes the model fit into the height observations [45]. The area under the logistic curve, AUC_L, was calculated to quantify each crop's overall cumulative growth.

2.3. Multispectral Image Collection and Processing

Multispectral images were collected using a Survey 3W Camera RGN (MAPIR Inc., San Diego, CA, USA), which can capture green (550 nm), red (660 nm), and near-infrared (850 nm) spectral wavelengths. The camera was mounted at the top of a tower to cover all 32 plants (2 plant species \times 4 treatments \times 4 replicates) in a single image. The images were collected between noon and 1:00 p.m. every day during the experimental period to minimize the effect of shadow, sun angle, and atmospheric conditions. For radiometric calibration, an image of a ground target, including four different reflectance panels (2%, 21%, 27%, and 83%), was collected each time the multispectral images were taken.

The raw images were pre-processed to convert the pixel values (digital number) to the spectral reflectance. A normalized difference vegetation index (NDVI) value was calculated from the processed images: Equation (3) [46,47].

$$\text{NDVI} = \frac{\rho_{\text{NIR}} - \rho_{\text{R}}}{\rho_{\text{NIR}} + \rho_{\text{R}}}, \quad \rho_{\text{NIR}} + \rho_{\text{R}} \neq 0, \quad (3)$$

where ρ_{NIR} is the near-infrared reflectance that has the center wavelength of 850 nm, and ρ_{R} represents the red band's reflectance with the center wavelength of 660 nm. Images that included anomalies or systematic errors were excluded from the analysis. A polygon (or an area of interest, AOI) was manually drawn to select pixels covering each plant's leaf canopy (Figure 2a). The angular sizes of the AOIs varied according to the distance between the sensor and plants. Any pixels with NDVI values smaller than 0.3 were screened out to make sure that only leaf pixels within an AOI were selected (Figure 2b), and the NDVI values of selected pixels (>15,000) within the AOI were averaged as the representative daily NDVI value. The statistical significance of differences in the vegetation growth statistics and index values, including relative and intrinsic growth rates, above-ground biomass, and NDVI values were determined with a one-way analysis of variance (ANOVA), and a post hoc Tukey's honestly significant difference (HSD) test was performed to identify a significant differences among treatments.

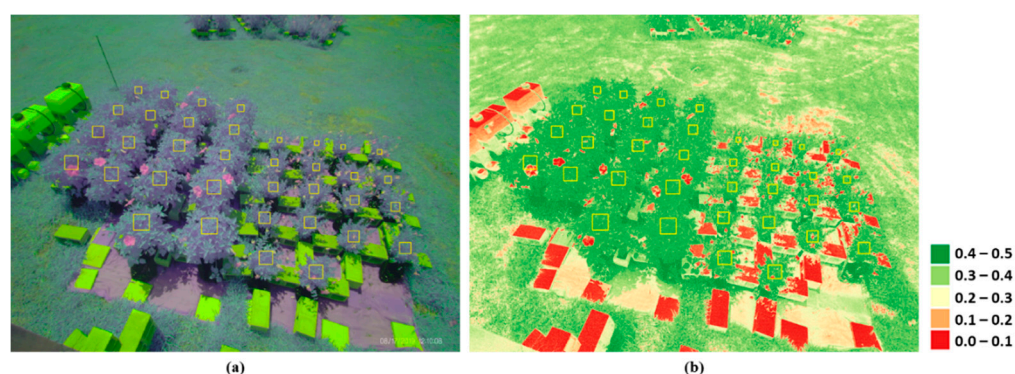


Figure 2. Examples of (a) false color and (b) NDVI images obtained from an image collected on 17 August 2019. The boxes in yellow indicate AOIs for the individual plants.

3. Results

3.1. Height and Above-Ground Biomass

Preliminary visual observations did not find apparent differences in the shapes and colors among plants treated with the salinity concentrations equal to or less than 4.0 dS/m (Figure 3a,c). The differences in visible symptoms were apparent between plants in the 7.0 and 10.0 dS/m treatments and plants in the other treatments. *H. rosa-sinensis* in the high salinity treatments had fewer leaves than those in the lower salinity treatments, whereas the leaves and flowers of *M. splendens* were wilted and/or necrotic in the high salinity treatments. Both crops were visibly wilted in the 10.0 dS/m treatment.

For *H. rosa-sinensis*, the control treatment had the highest RGR, and the RGR generally decreased as salinity concentration increased, especially in the second experiment (Figure 4). When irrigation water with the salinity concentrations of 1.5 (T2) and 2.0 dS/m (T3) was applied, the average RGRs of *M. splendens* were higher than that of the controls. The average RGR of *H. rosa-sinensis* and *M. splendens* substantially decreased when the salinity concentrations reached 7.0 and 4.0 dS/m, respectively, which could not be found in the visual assessment results (Figure 3).



Figure 3. Visual comparison between plants treated with the different irrigation water salinity concentrations. (a,b) *H. rosa-sinensis*; (c,d) *M. splendens*; (a,c) first experiment, Control: 0.5 dS/m, T1 1.0 dS/m, T2: 1.5 dS/m, T3: 2.0 dS/m; and (b,d) second experiment, Control: 0.5 dS/m, T4: 4.0 dS/m T5: 7.0 dS/m, T6: 10.0 dS/m.

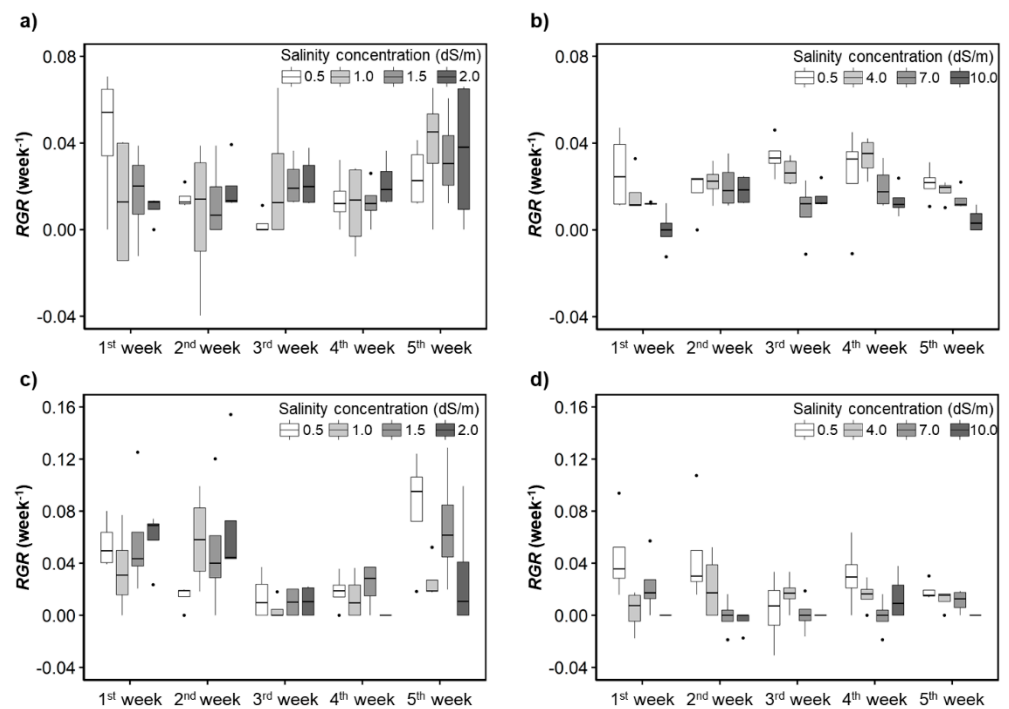


Figure 4. Responses of the relative growth rates (RGRs) to the irrigation water salinity levels. (a,b) *H. rosa-sinensis*; (c,d) *M. splendens*; (a,c) first experiment; (b,d) second experiment.

In the first experiment, the RGR of the control treatment for *H. rosa-sinensis* quickly decreased until the 4th week of the treatment and then started increasing from the 5th week (Figure 4a,b). The RGR_{max} (RGR obtained under the optimal growth conditions

or the highest RGR among the replicates) [48] of plants of each species in the control treatment was positively but weakly correlated ($r = 0.29$ for *H. rosa sinensis* and $r = 0.13$ for *M. splendens*) with changes in the air temperature. In the second experiment, there was also a positive correlation between the RGR_{max} and the air temperature changes for both plant species. Still, the correlation coefficients were stronger in the second experiment ($r = 0.73$ for *H. rosa sinensis* and $r = 0.47$ for *M. splendens*) than in the first experiment.

The RGR of plants treated with water that had salinity concentrations of 7.0 dS/m (T5) and 10.0 dS/m (T6) was significantly lower than that of the other treatments (Figure 4b,d). When the salinity concentrations were equal to or greater than 7.0 dS/m, the average RGR of the *M. splendens* was close to zero or even negative in the third week in the second experiment.

The largest above-ground biomass of both plant species was in the control treatment, except for the case of T4 for *H. rosa-sinensis* (in the second experiment) (Figure 5). In general, the above-ground biomass decreased with increased irrigation water salinity concentrations in both experiments, which was similar to the trends found for plant height. Plant height was correlated with above-ground biomass ($r = 0.91$ for the *H. rosa-sinensis* and $r = 0.73$ for the *M. splendens*). When the salinity concentration was equal to or greater than 7.0 dS/m for *H. rosa-sinensis* and 4.0 dS/m for *M. splendens*, the average above-ground biomass of the two crops declined rapidly.

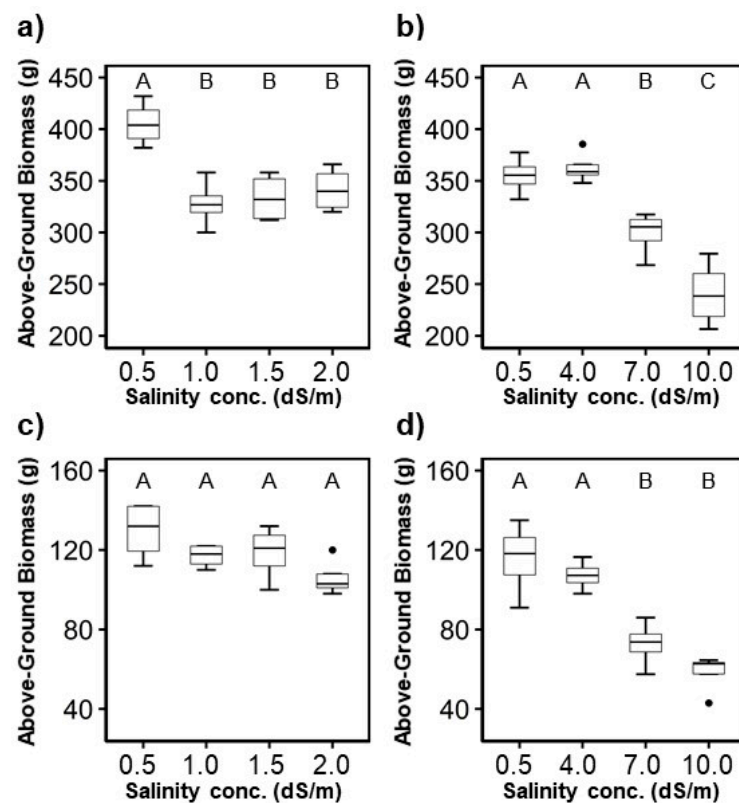


Figure 5. Variation of the above-ground biomass: (a,b) *H. rosa-sinensis*; (c,d) *M. splendens*; (a,c) first experiment; (b,d) second experiment. The boxplot's height represents the interquartile range (between the 75th and 25th percentiles), and the ends of the error bars signify the maximum and minimum values. Circles beyond the error bars are outliers. The same letters in a figure indicate that treatments were not significantly different at the $p < 0.05$ level by Tukey's HSD test.

The heights of the crops measured over time were fitted to logistic regression models to calculate their IGR and compare them (Figure 6). For *H. rosa sinensis*, there was no significant difference between the IGR of the control and the 7.0 and 10.0 dS/m salinity treatments. For *M. splendens*, the IGR was significantly lower when the salinity concentra-

tions reached 7.0 and 10.0 dS/m compared to the IGR of the control treatment ($p < 0.05$). The highest IGR was observed in the control treatments, except for the control treatment of *M. splendens* in the first experiment (Figure 6). Generally, the highest IGR observed in each treatment decreased as the salinity concentration increased. The highest IGR were also found in the control treatments, except for the *M. splendens* in the first experiment (Figure 6). A significant decreasing trend of IGR as salinity increased was only found when the salinity levels were increased from 0.5 to 4.0, 7.0, and 10.0 dS/m ($p < 0.05$).

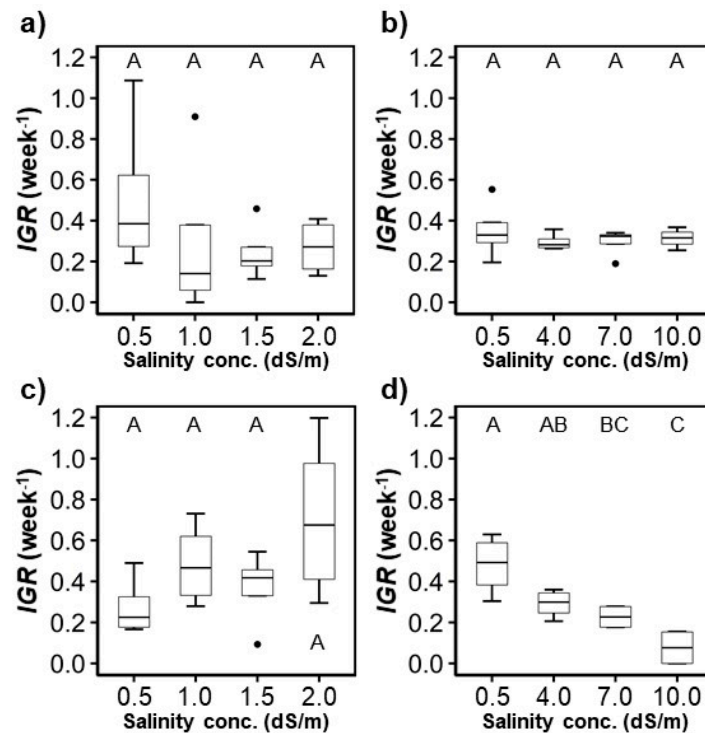


Figure 6. Variation of the intrinsic growth rate (IGR) provided by the fitted logistic growth models: (a,b) *H. rosa-sinensis*; (c,d) *M. splendens*; (a,c) first experiment; (b,d) second experiment. The same upper-case letters in a figure indicate they are not significantly different at the $p < 0.05$ level by Tukey's HSD test.

3.2. Remotely Sensed Vegetation Index

The NDVI values of *H. rosa-sinensis* treated with irrigation water that had varying salinity levels were statistically different from each other in most treatments of the second experiment (Figure 7a,b). In addition, the NDVI of T5 (7.0 dS/m) was not significantly different from that of T6 (10.0 dS/m). For *M. splendens*, the daily NDVI values over all treatments were not statistically different from each other (Figure 7c,d). Such a finding does not agree with the crop height and above-ground biomass measurements, indicating that the RGN sensor used to sense the crop vigorousness remotely might not be sensitive enough to detect the physiological changes of *M. splendens* in response to the salinity levels.

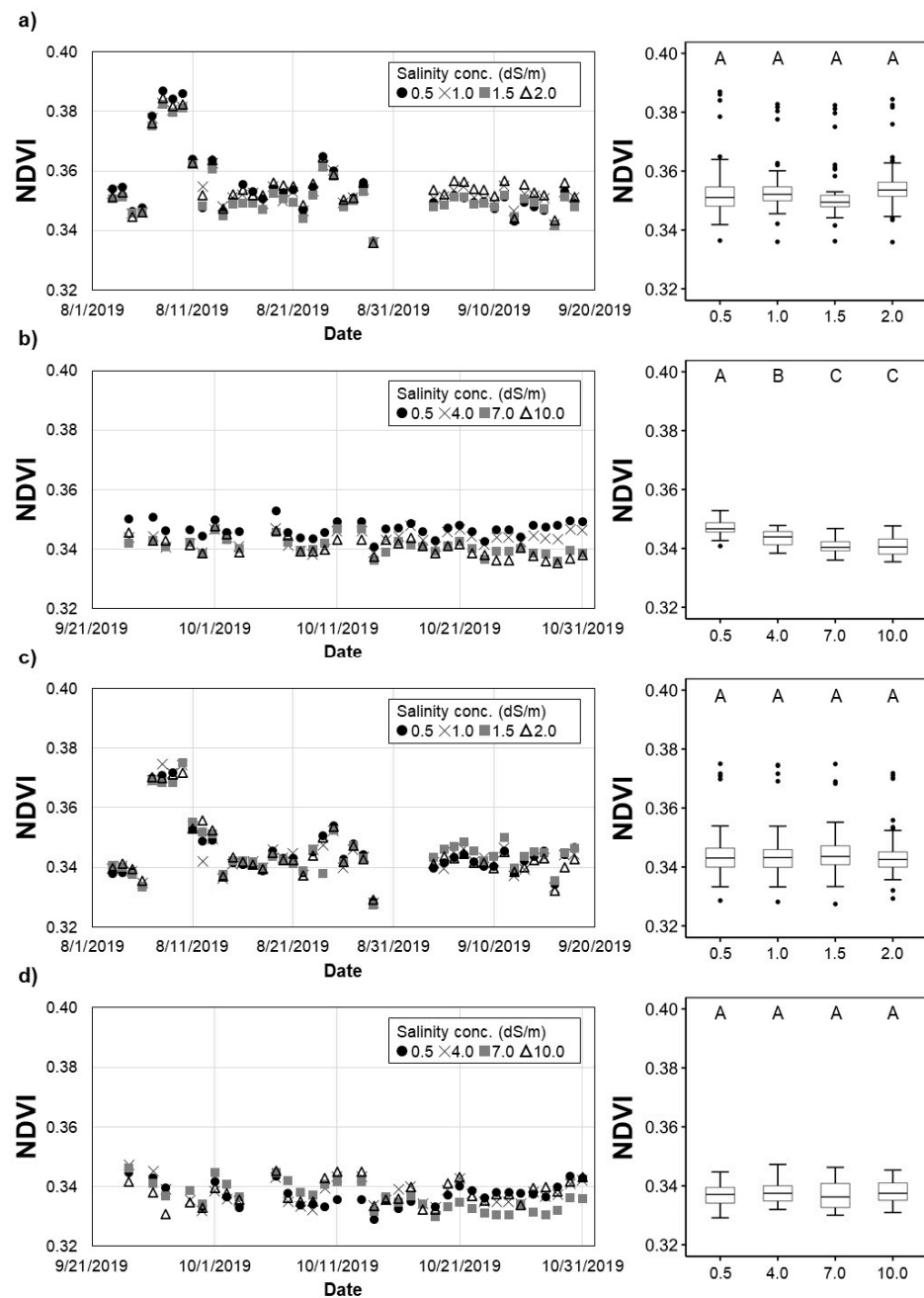


Figure 7. Variation of the NDVI: (a,b) *H. rosa-sinensis*; (c,d) *M. splendens*; (a,c) first experiment; (b,d) second experiment. The same upper-case letters in a figure indicate they are not significantly different at the $p < 0.05$ level by Tukey’s HSD test.

4. Discussion

The remotely sensed data agreed with the height and above-ground biomass measurements in terms of the impacts of irrigation water salinity on only one (*H. rosa-sinensis*) of the plant species studied, demonstrating the limitations and potential of remote sensing techniques used in this study. The analysis of remotely sensed data showed that NDVI was able to detect the changes in the vigor of *H. rosa-sinensis* in response to the different salinity treatments. Such a finding suggests that the combination of remote sensing and traditional monitoring methods would be more efficient and effective in crop health and salinity stress monitoring.

The daily NDVI values of the crops ranged from 0.33 to 0.39, which can be regarded as low, compared to those of other crop species [49–52]. The RGN images were taken at the

same time (noon) and location (in the northern right-hand corner of the field) every day during the experiments to minimize the impacts of daily weather variations. Wavelengths longer than visible light, such as near-infrared, are sensitive to the moisture content in the atmosphere and vegetation. An NDVI value is calculated as the ratio of the near-infrared and red band wavelengths. Vegetation index values tend to increase with increases in vegetation water contents because water more readily reflects the longer wavelength radiation [53]. The weather variables, including temperature, precipitation, and relative humidity of the air, might also have affected the signal captured on the sensor, even though the distance between the sensor and crops was short (3.5 m to 6.5 m) [54]. In this study, the association between NDVI and the weather variables was not strong ($r < 0.35$) on a daily basis (Figures 7 and 8). Such findings suggest the need for further evaluation of the accuracy and applicability of vegetation indices and remote sensing techniques in the vigorousness assessment of nursery crops.

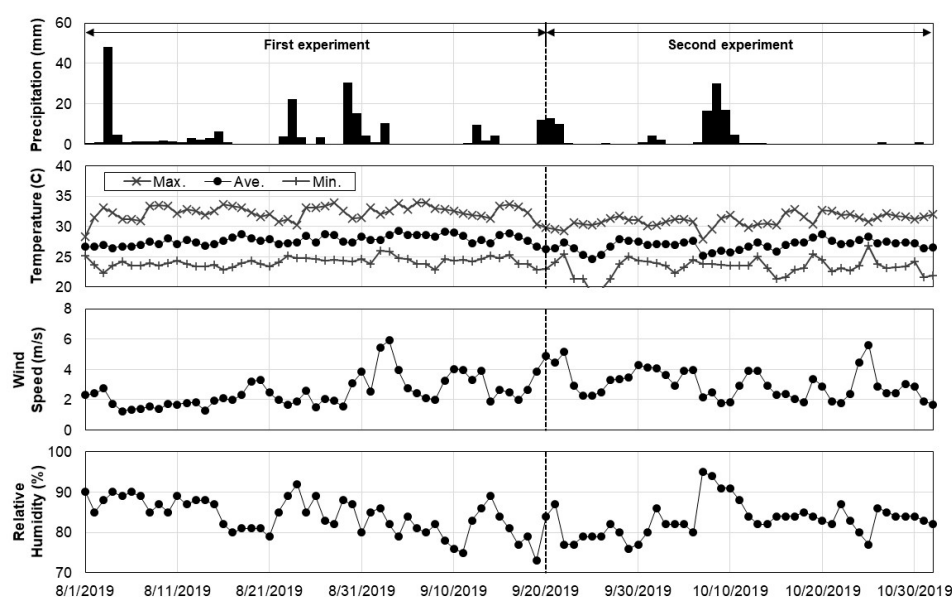


Figure 8. Daily time-series of precipitation, temperature, wind speed, and relative humidity.

A multi-spectral sensor (Survey 3W Camera RGN: MAPIR Inc., San Diego, CA, USA) was deployed at a 3.2-m height above the ground to capture the spectral characteristics of the plants' leaves directly exposed to the sensor. Thus, changes in the numbers and densities of leaves under the surface leaf layers might not be detected by the spectral sensor. Infrared temperature sensing can complement the spectral monitoring by differentiating leaves with relatively high stress due to increased irrigation water salinity. The limitation of the sensor itself might also be another cause of the insensitive responses of *M. splendens* to the salinity level changes (Figure 7c,d). Studies demonstrated the capacity of a low-cost sensor, such as one used in this study (Survey 3W), as an efficient tool to monitor plant growth and vegetation health [55–57]. However, low-cost sensors are known to be less sensitive to reflected radiation (low radiometric resolution) compared to high-end ones [58]. In addition, low-cost sensors tend to include more noisy spectral signals (low signal-to-noise ratio) due to the limited radiometric and spectral calibration of the sensors [58–60]. The radiometric calibration and manual AOI definition must be the sources of uncertainty in NDVI values, even though they were implemented in a consistent manner throughout the experiments. Studies showed that radiometric calibration results, including background noises and errors, are a function of atmospheric conditions and materials used to build a reflectance panel, and the image classification accuracy is affected by the selection of AOI [61–65]. Standard radiometric calibration procedures and automatic AOI definition procedures independent of images would help to reduce errors in the analysis.

Plant responses to salinity involve complicated (physiological, biochemical, and morphological) processes, and they can be observed in different plant organs and tissues [66,67]. Previous studies investigated the responses of various ornamental plants to saline irrigation water [68,69]. Visual quality ratings have been used to evaluate changes in ornamental crops' appearance, primarily focusing on foliage areas, colors, and shapes, in response to saline stress [68,70,71]. In the present study, the treated plants' appearance was visually investigated and compared with that of the control (0.5 dS/m). The visual examination provided salinity stress assessment results similar to those of the growth analysis with plant heights, widths, biomasses, and spectral characteristics. Still, it was not precise enough to detect small differences in the treated plants' responses (7.0 and 4.0 dS/m). Such a result suggests that plant responses to saline water can be more accurately monitored by growth analysis indices such as NDVI, RGR, IGR, and above-ground biomass. However, the visual quality of ornamental plants is critical to their market value. Changes in the aesthetic quality of plants may not be directly associated with those of biomass and growth variables [71]. Thus, the impacts of increased irrigation water salinity on the ornamental industry will be more accurately evaluated with quantitative and objective quality assessment methods customized for each type of ornamental plant [72,73].

Ornamental plants have different salinity tolerance levels. Niu and Rodriguez [70] showed that *G. rigens* and *D. Cooperi* were tolerant to the irrigation salinity levels of up to 12 dS/m. However, *Penstemon* species and *L. angustifolia* were not salt-tolerant, and died at 3.2 dS/m. Sun et al. [74] found that pomegranate plants were tolerant to salinity levels of up to 15 dS/m, and Sun et al. [75] observed that the visual quality of marigold was not substantially degraded at different irrigation water salinity levels of 3.0 and 6.0 dS/m depending on the cultivar. The salinity tolerance levels of *H. rosa-sinensis* and *M. splendens* found in the present study are within the ranges of those observed in previous studies. Zollinger et al. [71] tested the salt tolerance of the ornamental plants investigated by Niu and Rodriguez [70] in different seasons. They found that solar radiation and air temperatures affected the response of some of the plants to the salinity levels, and the elevated salinity levels more severely degraded their visual quality during warmer seasons than cooler months. The study by Zollinger et al. [71] implied that the plants' responses to the relatively high salinity levels in the second experiment (late September to late October) of this study could be more significant in summer.

5. Conclusions

This study investigated how the growth of two major nursery crops in south Florida, *H. rosa-sinensis* and *M. splendens*, responded to the different levels of irrigation water salinity. The results show that the current average level (the control of 0.5 dS/m) of groundwater salinity is safe for both plant species. *H. rosa-sinensis* was more tolerant to high irrigation water salinity levels than *M. splendens*. The plant growth and vigorousness were significantly limited when the salinity concentrations increased to 7.0 dS/m or greater. This implies that the reported maximum groundwater (irrigation water sources) salinity concentration of 9.12 dS/m along the coastal areas of south Florida can result in salinity stress and damage to nursery crops. Such a finding highlights the need to monitor the salinity levels and prepare groundwater salinity mitigation plans under the projected increases in sea level and the resulting increases in the frequency and severity of saltwater intrusion in south Florida.

Author Contributions: Conceptualization, Y.H. and E.V.C.; methodology, X.Y., Y.H., E.V.C. and B.S.; software, X.Y., A.C. and J.-H.S.; validation, X.Y., Y.H., A.C., J.-H.S. and B.S.; formal analysis, X.Y. and J.-H.S.; investigation, X.Y., Y.H., A.C., J.-H.S. and B.S.; resources, Y.H. and E.V.C.; data curation, X.Y., A.C. and J.-H.S.; writing—original draft preparation, X.Y., Y.H., A.C. and J.-H.S.; writing—review and editing, Y.H., E.V.C. and B.S.; visualization, X.Y. and J.-H.S.; supervision, Y.H.; project administration, Y.H.; funding acquisition, Y.H. and E.V.C. All authors have read and agreed to the published version of the manuscript.

Funding: This work was supported by the USDA National Institute of Food and Agriculture, Hatch project FLA-TRC-005551 and the Florida Department of Agriculture and Consumer Services, Best Management Practice Mini-grant program.

Institutional Review Board Statement: Not applicable.

Informed Consent Statement: Not applicable.

Data Availability Statement: Available upon request.

Conflicts of Interest: The authors declare no conflict of interest.

References

1. USDA-NASS United States Department of Agriculture-National Agricultural Statistics Service 2016. Available online: https://www.nass.usda.gov/Publications/Ag_Statistics/2016/index.php (accessed on 9 December 2019).
2. Parsons, L.R. Agricultural Use of Reclaimed Water in Florida: Food for Thought. *J. Contemp. Water Res. Educ.* **2018**, *165*, 20–27. [CrossRef]
3. Parsons, L.R.; Sheikh, B.; Holden, R.; York, D.W. Reclaimed Water as an Alternative Water Source for Crop Irrigation. *HortScience* **2010**, *45*, 1626–1629. [CrossRef]
4. FDACS Registered Nurseries and Stock Dealers 2019. Available online: <https://www.fdacs.gov/Agriculture-Industry> (accessed on 9 December 2019).
5. Bloetscher, F.; Heimlich, B.N.; Romah, T. Counteracting the Effects of Sea Level Rise in Southeast Florida. *J. Environ. Sci. Eng.* **2011**, *5*, 1507–1525.
6. Southeast Florida Regional Climate Change Compact Sea Level Rise Work Group (Compact) Unified Sea Level Rise Projection for Southeast Florida. Available online: <https://southeastfloridaclimatecompact.org/wp-content/uploads/2015/10/2015-Compact-Unified-Sea-Level-Rise-Projection.pdf> (accessed on 18 December 2019).
7. Trimble, P.J.; Santee, E.R.; Neidrauer, C.J. Preliminary Estimate of Impacts of Sea-Level Rise on the Regional Water Resources of Southeastern Florida. *J. Coast. Res.* **1998**, *26*, 252–255.
8. Marella, R.L. *Water Withdrawals in Florida, 2012: U.S. Geological Survey Open-File Report 2015–1156*; US Department of the Interior, US Geological Survey: Reston, VA, USA, 2015; p. 10.
9. Jiang, J.; DeAngelis, D.L.; Anderson, G.H.; Smith, T.J. Analysis and Simulation of Propagule Dispersal and Salinity Intrusion from Storm Surge on the Movement of a Marsh–Mangrove Ecotone in South Florida. *Estuaries Coasts* **2014**, *37*, 24–35. [CrossRef]
10. Park, J.; Obeysekera, J.; Irizarry, M.; Barnes, J.; Trimble, P.; Park-Said, W. Storm Surge Projections and Implications for Water Management in South Florida. *Clim. Chang.* **2011**, *107*, 109–128. [CrossRef]
11. Kussul, N.; Lavreniuk, M.; Skakun, S.; Shelestov, A. Deep Learning Classification of Land Cover and Crop Types Using Remote Sensing Data. *IEEE Geosci. Remote Sens. Lett.* **2017**, *14*, 778–782. [CrossRef]
12. Salmon, J.M.; Friedl, M.A.; Frohling, S.; Wisser, D.; Douglas, E.M. Global Rain-Fed, Irrigated, and Paddy Croplands: A New High Resolution Map Derived from Remote Sensing, Crop Inventories and Climate Data. *Int. J. Appl. Earth Obs. Geoinf.* **2015**, *38*, 321–334. [CrossRef]
13. Shakoor, N.; Northrup, D.; Murray, S.; Mockler, T.C. Big Data Driven Agriculture: Big Data Analytics in Plant Breeding, Genomics, and the Use of Remote Sensing Technologies to Advance Crop Productivity. *Plant Phenome J.* **2019**, *2*, 1–9. [CrossRef]
14. Huang, Y.; Chen, Z.; Yu, T.; Huang, X.; Gu, X. Agricultural Remote Sensing Big Data: Management and Applications. *J. Integr. Agric.* **2018**, *17*, 1915–1931. [CrossRef]
15. Jin, X.; Kumar, L.; Li, Z.; Feng, H.; Xu, X.; Yang, G.; Wang, J. A Review of Data Assimilation of Remote Sensing and Crop Models. *Eur. J. Agron.* **2018**, *92*, 141–152. [CrossRef]
16. Kasampalis, D.A.; Alexandridis, T.K.; Deva, C.; Challinor, A.; Moshou, D.; Zalidis, G. Contribution of Remote Sensing on Crop Models: A Review. *J. Imaging* **2018**, *4*, 52. [CrossRef]
17. Cao, L.; Liu, K.; Shen, X.; Wu, X.; Liu, H. Estimation of Forest Structural Parameters Using UAV-LiDAR Data and a Process-Based Model in Ginkgo Planted Forests. *IEEE J. Sel. Top. Appl. Earth Obs. Remote Sens.* **2019**, *12*, 4175–4190. [CrossRef]
18. Mtui, Y.P.; Erdbrügger, J.; Hussin, Y.A.; Leeuwen, L.M.V.; Kloosterman, E.H.; Ismail, M.H. Comparison of Forest Tree Parameters Extracted from Uav Optical and Tls Data in Both Tropical Rain and Temperate Forests. In Proceedings of the 38th Asian Conference on Remote Sensing 2017: Space Applications: Touching Human Lives, New Delhi, India, 1 January 2017.
19. Ashapure, A.; Jung, J.; Yeom, J.; Chang, A.; Maeda, M.; Maeda, A.; Landivar, J. A Novel Framework to Detect Conventional Tillage and No-Tillage Cropping System Effect on Cotton Growth and Development Using Multi-Temporal UAS Data. *ISPRS J. Photogramm. Remote Sens.* **2019**, *152*, 49–64. [CrossRef]
20. Doughty, C.L.; Cavanaugh, K.C. Mapping Coastal Wetland Biomass from High Resolution Unmanned Aerial Vehicle (UAV) Imagery. *Remote Sens.* **2019**, *11*, 540. [CrossRef]
21. Ivushkin, K.; Bartholomeus, H.; Bregt, A.K.; Pulatov, A.; Franceschini, M.H.D.; Kramer, H.; van Loo, E.N.; Jaramillo Roman, V.; Finkers, R. UAV Based Soil Salinity Assessment of Cropland. *Geoderma* **2019**, *338*, 502–512. [CrossRef]

22. Guan, S.; Fukami, K.; Matsunaka, H.; Okami, M.; Tanaka, R.; Nakano, H.; Sakai, T.; Nakano, K.; Ohdan, H.; Takahashi, K. Assessing Correlation of High-Resolution NDVI with Fertilizer Application Level and Yield of Rice and Wheat Crops Using Small UAVs. *Remote Sens.* **2019**, *11*, 112. [[CrossRef](#)]
23. Hassan, M.A.; Yang, M.; Rasheed, A.; Yang, G.; Reynolds, M.; Xia, X.; Xiao, Y.; He, Z. A Rapid Monitoring of NDVI across the Wheat Growth Cycle for Grain Yield Prediction Using a Multi-Spectral UAV Platform. *Plant Sci.* **2019**, *282*, 95–103. [[CrossRef](#)]
24. Brede, B.; Suomalainen, J.; Roosjen, P.; Aasen, H.; Kooistra, L.; Bartholomeus, H.; Clevers, J.; Herold, M. *Opportunities of UAV Based Sensing for Vegetation Land Product Validation*; European Space Agency: Rome, Italy, 2018.
25. González-Jaramillo, V.; Fries, A.; Bendix, J. AGB Estimation in a Tropical Mountain Forest (TMF) by Means of RGB and Multispectral Images Using an Unmanned Aerial Vehicle (UAV). *Remote Sens.* **2019**, *11*, 1413. [[CrossRef](#)]
26. Guo, X.; Wang, L.; Tian, J.; Yin, D.; Shi, C.; Nie, S. Vegetation Horizontal Occlusion Index (VHOI) from TLS and UAV Image to Better Measure Mangrove LAI. *Remote Sens.* **2018**, *10*, 1739. [[CrossRef](#)]
27. Li, S.; Yuan, F.; Ata-UI-Karim, S.T.; Zheng, H.; Cheng, T.; Liu, X.; Tian, Y.; Zhu, Y.; Cao, W.; Cao, Q. Combining Color Indices and Textures of UAV-Based Digital Imagery for Rice LAI Estimation. *Remote Sens.* **2019**, *11*, 1763. [[CrossRef](#)]
28. Alberton, B.; Torres, R.d.S.; Cancian, L.F.; Borges, B.D.; Almeida, J.; Mariano, G.C.; dos Santos, J.; Morellato, L.P.C. Introducing Digital Cameras to Monitor Plant Phenology in the Tropics: Applications for Conservation. *Perspect. Ecol. Conserv.* **2017**, *15*, 82–90. [[CrossRef](#)]
29. Brocks, S.; Bareth, G. Estimating Barley Biomass with Crop Surface Models from Oblique RGB Imagery. *Remote Sens.* **2018**, *10*, 268. [[CrossRef](#)]
30. Enciso, J.; Maeda, M.; Landivar, J.; Jung, J.; Chang, A. A Ground Based Platform for High Throughput Phenotyping. *Comput. Electron. Agric.* **2017**, *141*, 286–291. [[CrossRef](#)]
31. Hall, F.G.; Hilker, T.; Coops, N.C. PHOTOSYN SAT, Photosynthesis from Space: Theoretical Foundations of a Satellite Concept and Validation from Tower and Spaceborne Data. *Remote Sens. Environ.* **2011**, *115*, 1918–1925. [[CrossRef](#)]
32. Naito, H.; Ogawa, S.; Valencia, M.O.; Mohri, H.; Urano, Y.; Hosoi, F.; Shimizu, Y.; Chavez, A.L.; Ishitani, M.; Selvaraj, M.G.; et al. Estimating Rice Yield Related Traits and Quantitative Trait Loci Analysis under Different Nitrogen Treatments Using a Simple Tower-Based Field Phenotyping System with Modified Single-Lens Reflex Cameras. *ISPRS J. Photogramm. Remote Sens.* **2017**, *125*, 50–62. [[CrossRef](#)]
33. Lyons, J.M. Chilling Injury in Plants. *Annu. Rev. Plant Physiol.* **1973**, *24*, 445–466. [[CrossRef](#)]
34. Paredes, M.; Quiles, M.J. The Effects of Cold Stress on Photosynthesis in Hibiscus Plants. *PLoS ONE* **2015**, *10*, e0137472. [[CrossRef](#)]
35. Hughes, J.D.; White, J.T. *Hydrologic Conditions in Urban Miami-Dade County, Florida, and the Effect of Groundwater Pumpage and Increased Sea Level on Canal Leakage and Regional Groundwater Flow*; U.S. Department of the Interior, U.S. Geological Survey: Reston, VA, USA, 2016; 175p.
36. USGS USGS Water Data for the Nation 2019. Available online: <https://waterdata.usgs.gov/nwis> (accessed on 9 December 2019).
37. Miami-Dade County Board of County Commissioners. *Report on Flooding and Salt Water Intrusion*; Miami-Dade County Board of County Commissioners: Miami-Dade County, FL, USA, 2016.
38. Hilbert, D.W.; Swift, D.M.; Detling, J.K.; Dyer, M.I. Relative Growth Rates and the Grazing Optimization Hypothesis. *Oecologia* **1981**, *51*, 14–18. [[CrossRef](#)] [[PubMed](#)]
39. Radford, P.J. Growth Analysis Formulae—Their Use and Abuse. *Crop Sci.* **1967**, *7*, 171–175. [[CrossRef](#)]
40. Deng, J.; Ran, J.; Wang, Z.; Fan, Z.; Wang, G.; Ji, M.; Liu, J.; Wang, Y.; Liu, J.; Brown, J.H. Models and Tests of Optimal Density and Maximal Yield for Crop Plants. *Proc. Natl. Acad. Sci. USA* **2012**, *109*, 15823–15828. [[CrossRef](#)]
41. Liu, J.-H.; Yan, Y.; Ali, A.; Yu, M.-F.; Xu, Q.-J.; Shi, P.-J.; Chen, L. Simulation of Crop Growth, Time to Maturity and Yield by an Improved Sigmoidal Model. *Sci. Rep.* **2018**, *8*, 7030. [[CrossRef](#)] [[PubMed](#)]
42. Paine, C.E.T.; Marthews, T.R.; Vogt, D.R.; Purves, D.; Rees, M.; Hector, A.; Turnbull, L.A. How to Fit Nonlinear Plant Growth Models and Calculate Growth Rates: An Update for Ecologists. *Methods Ecol. Evol.* **2012**, *3*, 245–256. [[CrossRef](#)]
43. Sprouffske, K.; Wagner, A. Growthcurver: An R Package for Obtaining Interpretable Metrics from Microbial Growth Curves. *Bmc Bioinform.* **2016**, *17*, 172. [[CrossRef](#)] [[PubMed](#)]
44. Zeide, B. Analysis of Growth Equations. *For. Sci.* **1993**, *39*, 594–616. [[CrossRef](#)]
45. Kheloufi, N.; Kahlouche, S.; Lamara, R.A.A. *Non Linear Least Squares(Levenberg-Marquardt Algorithms) for Geodetic Adjustment and Coordinates Transformation*; European Geosciences Union: Vienna, Austria, 2009; Volume 11, p. 333.
46. Carlson, T.N.; Ripley, D.A. On the Relation between NDVI, Fractional Vegetation Cover, and Leaf Area Index. *Remote Sens. Environ.* **1997**, *62*, 241–252. [[CrossRef](#)]
47. Rouse, J.W.; Haas, R.H.; Schell, J.A.; Deering, D.W. Monitoring Vegetation Systems in the Great Plains with ERTS. *NASA Spec. Publ.* **1974**, *351*, 309.
48. Grime, J.P.; Hunt, R. Relative Growth-Rate: Its Range and Adaptive Significance in a Local Flora. *J. Ecol.* **1975**, *63*, 393–422. [[CrossRef](#)]
49. Liu, X.; Bo, Y.; Zhang, J.; He, Y. Classification of C3 and C4 Vegetation Types Using MODIS and ETM+ Blended High Spatio-Temporal Resolution Data. *Remote Sens.* **2015**, *7*, 15244–15268. [[CrossRef](#)]
50. Naser, M.A.; Khosla, R.; Longchamps, L.; Dahal, S. Using NDVI to Differentiate Wheat Genotypes Productivity Under Dryland and Irrigated Conditions. *Remote Sens.* **2020**, *12*, 824. [[CrossRef](#)]

51. Shen, M.; Chen, J.; Zhu, X.; Tang, Y.; Chen, X. Do Flowers Affect Biomass Estimate Accuracy from NDVI and EVI? *Int. J. Remote Sens.* **2010**, *31*, 2139–2149. [[CrossRef](#)]
52. Tieszen, L.L.; Reed, B.C.; Bliss, N.B.; Wylie, B.K.; DeJong, D.D. Ndvi, C3 and C4 Production, and Distributions in Great Plains Grassland Land Cover Classes. *Ecol. Appl.* **1997**, *7*, 59–78. [[CrossRef](#)]
53. Chen, D.; Huang, J.; Jackson, T.J. Vegetation Water Content Estimation for Corn and Soybeans Using Spectral Indices Derived from MODIS Near- and Short-Wave Infrared Bands. *Remote Sens. Environ.* **2005**, *98*, 225–236. [[CrossRef](#)]
54. Hao, F.; Zhang, X.; Ouyang, W.; Skidmore, A.K.; Toxopeus, A.G. Vegetation NDVI Linked to Temperature and Precipitation in the Upper Catchments of Yellow River. *Environ. Model Assess* **2012**, *17*, 389–398. [[CrossRef](#)]
55. Ren, D.D.W.; Tripathi, S.; Li, L.K.B. Low-Cost Multispectral Imaging for Remote Sensing of Lettuce Health. *J. Appl. Remote Sens.* **2017**, *11*, 016006. [[CrossRef](#)]
56. Dehm, D. A Small Unmanned Aerial System (SUAS) Based Method for Monitoring Wetland Inundation & Vegetation. Ph.D. Thesis, University of Toledo, Toledo, OH, USA, 2019.
57. Bahe, M. Nursery Production Method Performance Evaluation Assessed with the Normalized Difference Vegetation Index Derived from an Unmanned Aircraft System Mounted Single-Imager Sensor. Master's Thesis, University of Minnesota, Minneapolis, MN, USA, 2020.
58. Coburn, C.A.; Smith, A.M.; Logie, G.S.; Kennedy, P. Radiometric and Spectral Comparison of Inexpensive Camera Systems Used for Remote Sensing. *Int. J. Remote Sens.* **2018**, *39*, 4869–4890. [[CrossRef](#)]
59. Cucho-Padin, G.; Loayza, H.; Palacios, S.; Balcazar, M.; Carbajal, M.; Quiroz, R. Development of Low-Cost Remote Sensing Tools and Methods for Supporting Smallholder Agriculture. *Appl. Geomat.* **2020**, *12*, 247–263. [[CrossRef](#)]
60. Burggraaff, O.; Schmidt, N.; Zamorano, J.; Pauly, K.; Pascual, S.; Tapia, C.; Spyarakos, E.; Snik, F. Standardized Spectral and Radiometric Calibration of Consumer Cameras. *Opt. Express* **2019**, *27*, 19075–19101. [[CrossRef](#)]
61. Del Pozo, S.; Rodríguez-Gonzálvez, P.; Hernández-López, D.; Felipe-García, B. Vicarious Radiometric Calibration of a Multispectral Camera on Board an Unmanned Aerial System. *Remote Sens.* **2014**, *6*, 1918–1937. [[CrossRef](#)]
62. Iqbal, F.; Lucieer, A.; Barry, K. Simplified Radiometric Calibration for UAS-Mounted Multispectral Sensor. *Eur. J. Remote Sens.* **2018**, *51*, 301–313. [[CrossRef](#)]
63. Berhane, T.M.; Costa, H.; Lane, C.R.; Anenkhonov, O.A.; Chepinoga, V.V.; Autrey, B.C. The Influence of Region of Interest Heterogeneity on Classification Accuracy in Wetland Systems. *Remote Sens.* **2019**, *11*, 551. [[CrossRef](#)]
64. Guo, Y.; Senthilnath, J.; Wu, W.; Zhang, X.; Zeng, Z.; Huang, H. Radiometric Calibration for Multispectral Camera of Different Imaging Conditions Mounted on a UAV Platform. *Sustainability* **2019**, *11*, 978. [[CrossRef](#)]
65. Rosas, J.T.F.; de Carvalho Pinto, F.D.A.; Queiroz, D.M.D.; de Melo Villar, F.M.; Martins, R.N.; Silva, S.D.A. Low-Cost System for Radiometric Calibration of UAV-Based Multispectral Imagery. *J. Spat. Sci.* **2020**, *0*, 1–15. [[CrossRef](#)]
66. Flowers, T.J.; Colmer, T.D. Salinity Tolerance in Halophytes. *New Phytol.* **2008**, *179*, 945–963. [[CrossRef](#)]
67. Sperling, O.; Lazarovitch, N.; Schwartz, A.; Shapira, O. Effects of High Salinity Irrigation on Growth, Gas-Exchange, and Photoprotection in Date Palms (*Phoenix Dactylifera* L., Cv. Medjool). *Environ. Exp. Bot.* **2014**, *99*, 100–109. [[CrossRef](#)]
68. Cassaniti, C.; Romano, D.; Flowers, T.J. The response of ornamental plants to saline irrigation water. In *Irrigation: Water Management, Pollution and Alternative Strategies*; InTech: Rijeka, Croatia, 2012; pp. 131–158.
69. García-Caparrós, P.; Lao, M.T. The Effects of Salt Stress on Ornamental Plants and Integrative Cultivation Practices. *Sci. Hortic.* **2018**, *240*, 430–439. [[CrossRef](#)]
70. Niu, G.; Rodriguez, D.S. Relative Salt Tolerance of Selected Herbaceous Perennials and Groundcovers. *Sci. Hortic.* **2006**, *110*, 352–358. [[CrossRef](#)]
71. Zollinger, N.; Koenig, R.; Cerny-Koenig, T.; Kjelgren, R. Relative Salinity Tolerance of Intermountain Western United States Native Herbaceous Perennials. *HortScience* **2007**, *42*, 529–534. [[CrossRef](#)]
72. Garbez, M.; Belin, E.; Chéné, Y.; Dones, N.; Hunault, G.; Relion, D.; Sigogne, M.; Symoneaux, R.; Rousseau, D.; Galopin, G. A New Approach to Predict the Visual Appearance of Rose Bush from Image Analysis of 3D Videos. *Eur. J. Hortic. Sci.* **2020**, *85*, 182–190. [[CrossRef](#)]
73. Santagostini, P.; Demotes-Mainard, S.; Huché-Thélier, L.; Leduc, N.; Bertheloot, J.; Guérin, V.; Bourbeillon, J.; Sakr, S.; Boumaza, R. Assessment of the Visual Quality of Ornamental Plants: Comparison of Three Methodologies in the Case of the Rosebush. *Sci. Hortic.* **2014**, *168*, 17–26. [[CrossRef](#)]
74. Sun, Y.; Niu, G.; Masabni, J.G.; Ganjegunte, G. Relative Salt Tolerance of 22 Pomegranate (*Punica Granatum*) Cultivars. *HortScience* **2018**, *53*, 1513–1519. [[CrossRef](#)]
75. Sun, Y.; Niu, G.; Perez, C.; Pemberton, H.B.; Altland, J. Responses of Marigold Cultivars to Saline Water Irrigation. *HortTechnology* **2018**, *28*, 166–171. [[CrossRef](#)]